Inhibition of adenine nucleotide translocator pore function and protection against apoptosis in vivo by an HIV protease inhibitor

Joel G.R. Weaver,[1,2,3] Agathe Tarze,[4] Tia C. Moffat,[5] Morgane LeBras,[4] Aurelien Deniaud,[4] Catherine Brenner,[4] Gary D. Bren,[2] Mario Y. Morin,[5] Barbara N. Phenix,[3] Li Dong,[3,6] Susan X. Jiang,[7] Valerie L. Sim,[8] Bogdan Zurakowski,[7] Jessica Lallier,[5] Heather Hardin,[9] Peter Wettstein,[9] Rolf P.G. van Heeswijk,[3] Andre Douen,[3] Romano T. Kroemer,[10] Sheng T. Hou,[7] Steffany A.L. Bennett,[5] David H. Lynch,[11] Guido Kroemer,[12] and Andrew D. Badley[2,13]

[1]Division of General Surgery, University of Ottawa, Ottawa, Ontario, Canada. [2]Division of Infectious Diseases, Mayo Clinic and Foundation, Rochester, Minnesota, USA. [3]Ottawa Health Research Institute, University of Ottawa, Ottawa, Ontario, Canada. [4]Université de Versailles Saint-Quentin-en-Yvelines, Versailles, France. [5]Neural Regeneration Laboratory, Department of Biochemistry, Microbiology, and Immunology, and [6]Department of Pathology, University of Ottawa, Ottawa, Ontario, Canada. [7]Experimental Stroke Group, National Research Council Institute for Biological Sciences (NRC/IBS), National Research Council of Canada, Ottawa, Ontario, Canada. [8]Division of Neurology, Ottawa Hospital, Ottawa, Ontario, Canada. [9]Department of Surgery and Immunology, Mayo Clinic, Rochester, Minnesota, USA. [10]Sanofi Aventis, Centre de Recherche de Paris, Vitry-sur-Seine, France. [11]Amnis Corp., Seattle, Washington, USA. [12]Institut Gustave Roussy, Villejuif, France. [13]Translational Program in Immunology and Biodefense, Mayo Clinic and Foundation, Rochester, Minnesota, USA.

Inhibitors of HIV protease have been shown to have antiapoptotic effects in vitro, yet whether these effects are seen in vivo remains controversial. In this study, we have evaluated the impact of the HIV protease inhibitor (PI) nelfinavir, boosted with ritonavir, in models of nonviral disease associated with excessive apoptosis. In mice with Fas-induced fatal hepatitis, *Staphylococcal enterotoxin B*–induced shock, and middle cerebral artery occlusion–induced stroke, we demonstrate that PIs significantly reduce apoptosis and improve histology, function, and/or behavioral recovery in each of these models. Further, we demonstrate that both in vitro and in vivo, PIs block apoptosis through the preservation of mitochondrial integrity and that in vitro PIs act to prevent pore function of the adenine nucleotide translocator (ANT) subunit of the mitochondrial permeability transition pore complex.

Introduction

The abnormal regulation of apoptosis is thought to contribute to a variet of pathologic disease processes in vivo. HIV-induced CD4 T cell depletion and consequent immunodeficienc is one such disease state in which e cessive apoptosis has been implicated. Current therapies for HIV not onl reduce HIV replication but ma also directl impact apoptosis; indeed, man groups have now reported that HIV protease inhibitors (PIs) can inhibit apoptosis at concentrations similar to those that are commonl seen in the plasma of patients receiving such treatments (reviewed in ref. 1). Parado icall , such agents ma also induce apoptosis, particularl of transformed cells, when used at higher doses (2, 5).

Studies b several groups have investigated the potential mechanisms b which PIs ma inhibit apoptosis, ielding different results. Proposed mechanisms include altered transcriptional regulation of ke apoptosis regulator proteins (5, 7) and/or direct inhibition of the apoptosis en me ICE (8, 9) and/or calpain (10). Such theories cannot full account for the abilit of PIs to inhibit diverse apoptotic stimuli (reviewed in ref. 1) or the lack of en matic inhibition of recombinant caspases in vitro (11). According to another proposed mechanism to account for apoptosis inhibition, PIs alter the propensit of mitochondria to transduce apoptotic signals. This latter model is supported b the findings that PIs are able to block Fas-induced apoptosis involving mitochondrial signaling but not Fas-induced apoptosis that is mitochondria independent (11) and that PIs are able to rescue cells from apoptosis induced b mitochondrioto ic agents (5, 12).

Despite these in vitro findings, it remains controversial whether PI therap for HIV-infected patients offers additional benefits in terms of CD4 T cell reconstitution compared with non-PI, containing regimens of equal antiviral potenc (13, 14). Most studies that demonstrate enhanced CD4 T cell improvements in patients receiving PI therap were retrospective, post-hoc anal ses (15), which raises concerns about the methodologies used. Consequentl , at least one stud was designed to compare CD4 T cell number, activation profile, memor and naive T cell subsets, and apoptosis between patients receiving PI-continuing or PI-sparing regimens (16). No differences were observed between groups regarding CD4 T cell number, activation, or memor or naive subsets; however, within the first week of therap , significantl less apoptosis was seen in CD4 T cells of patients receiving PI therap than in patients who did not receive PI therap (16). Such data are consistent with the postulated antiapoptotic effects of PIs.

The objectives of this stud were, first, to evaluate whether PIs were antiapoptotic in vivo b evaluating apoptotic changes in animal models of disease that are associated with e cessive apopto-

Nonstandard abbreviations used: $\Delta\Psi_m$, membrane permeabilit ; ANT, adenine nucleotide translocator; AST, aspartate amino transferase; ATR, atract loside; D-gal, D-galactosamine; MCAO, middle cerebral arter occlusion; NFV, nelfinavir; PBR, ben odia epine receptor; PI, protease inhibitor; PTPC, permeabilit transition pore comple ; RIT, ritonavir; RT, room temperature; SEB, *Staphylococcal enterotoxin B*; STS, staurosporine; TTC, 2,3,5-triphen ltetra olium; VDAC, voltage-dependent anion channel.

Conflict of interest: The authors have declared that no conflict of interest e ists.

Citation for this article: *J. Clin. Invest.* **115**:1828 1838 (2005). doi:10.1172/JCI22954.

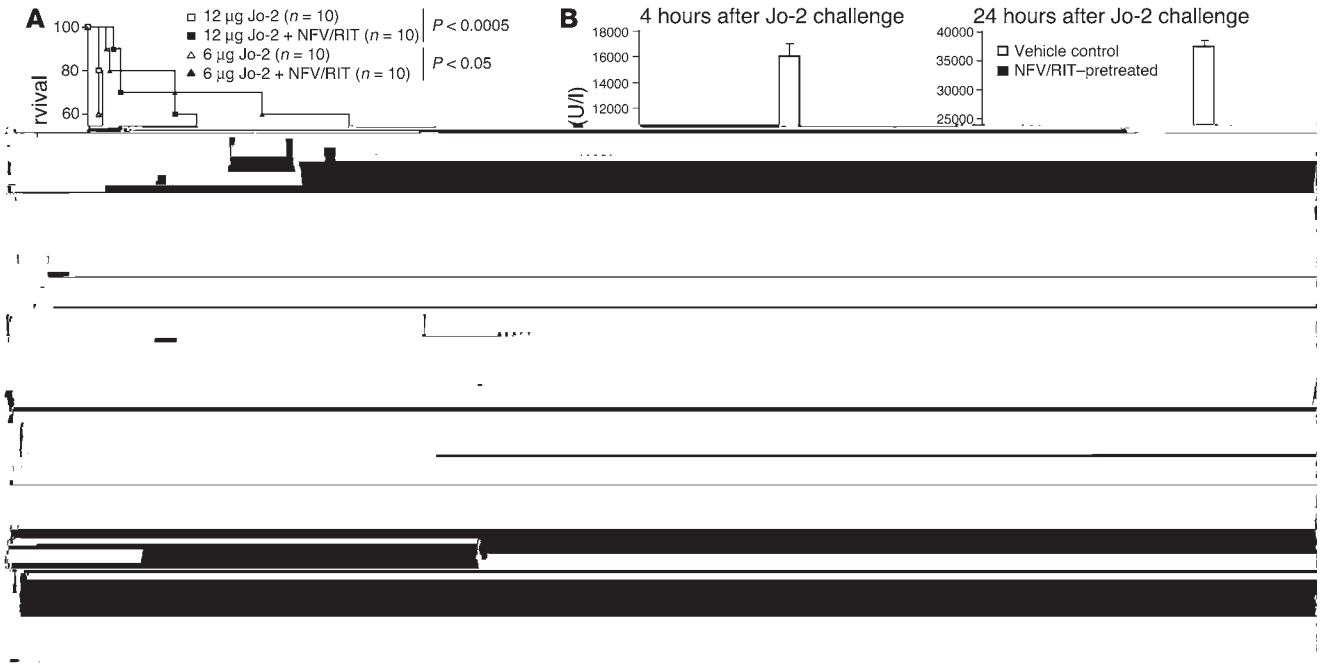

Figure 1

Effects of NFV/RIT on Jo-2–induced hepatitis or SEB-induced shock. (**A**) Mice treated with varying doses of Jo-2 antibody in the presence or absence of NFV/RIT were followed for 30 days and analyzed for survival. (**B**) In parallel, mice treated in a similar manner were sacrificed at 4 or 24 hours and analyzed for serum AST level. *$P < 0.05$. (**C**) Five mice per group were treated with SEB/D-gal with or without NFV/RIT before or 4 hours after SEB or with NFV alone or RIT alone before SEB. Twenty-four-hour survival was monitored (cumulative data from 4 independent experiments are shown). (**D**) Mice treated with SEB/D-gal with NFV/RIT or control were analyzed for V-β8 T cell apoptosis by TUNEL assay (cumulative data from 4 independent experiments are shown). #$P < 0.01$.

sis but that do not depend upon viral replication and, second, to evaluate the mechanisms involved.

Results

As mouse metabolism of PIs differs from that of humans, we first performed pharmacokinetic studies of mice treated with nelfinavir (NFV) at doses used in human therap . Within 1 hour of dosing, mice had undetectable levels of NFV. Therefore, we co-dosed mice with ritonavir (RIT), another PI known to increase PI levels in humans (17). Ultimatel , a dose of 125 mg/kg NFV and 13 mg/kg RIT resulted in drug levels similar to those of humans treated with NFV alone (see Methods). This dose was used for in vivo testing.

First, we evaluated the impact of NFV/RIT treatment on CD95/Fas-induced hepatic failure (18, 20). Mice received NFV/RIT or vehicle control pretreatment for 24 hours followed b treatment with 6 or 12 μg of IV Jo-2 anti-Fas antibod . Control animals died in a dose-dependent manner, whereas NFV/RIT-pretreated animals displa ed superior survival compared with controls (Figure 1A). Moreover, survival of mice treated with RIT (13 mg/kg) was similar to that of controls, which indicates that NFV was responsible for the observed improved survival. Importantl , all mice that died did so within 72 hours, which indicates that NFV/RIT trul prevents rather than dela s Jo-2, induced hepatoto icit and death. In parallel, groups of 10 mice received 2.5, 5, or 7.5 μg of IV Jo-2 with or without NFV/RIT pretreatment. Mice were sacrificed at 4 or 24 hours and anal ed for serum biochemistr , H&E histolog , and apoptosis b TUNEL staining. Serum glucose, blood urea nitrogen, creatinine, phosphorus, total protein, albumin, globulin, bilirubin, and cholesterol levels were similar in the 2 groups (data not shown). However, NFV/RIT-pretreated mice had attenuated elevations in serum aspartate amino transferase (AST) at both 4 and 24 hours compared with control mice ($P < 0.03$; Figure 1B), reduced evidence of hepatitis at 48 hours on H&E histolog , and a reduced quantit of TUNEL-positive hepatoc tes from a mean of 50% to 15% (measured in 5 mice per group; $P = 0.002$; data not shown).

To assess whether NFV/RIT protection e tended to other apoptotic disease processes, we treated mice with the bacterial superantigen *Staphylococcal enterotoxin B* (SEB) in the presence or absence of NFV/RIT. S stemic treatment with SEB results in shock and the selective apoptosis of V-β8 positive T cells (21). When coadministered with D-galactosamine (D-gal), SEB injection also results in death (22, 23). Following administration of SEB, apoptosis was measured b TUNEL assa in the V-β8 and V-β3 subsets of splenoc tes. Four hours following SEB treatment, 72.6% of V-β8 cells were TUNEL positive, whereas 21.7% of V-β3 cells were TUNEL positive ($n = 3$; $P < 0.05$), which indicates that SEB selectivel induced death in V-β8 cells. Parallel groups of mice were pretreated for 24 hours with NFV/RIT, vehicle control, NFV alone, or RIT alone, followed b treatment with 20 mg D-gal and 6.5 μg SEB. NFV/RIT-treated mice had improved survival compared with vehicle control (89%, $n = 9$ vs. 27%, $n = 11$; $P < 0.01$). Survival of vehicle-treated mice was not significantl different from that of mice treated with NFV alone (30%; $n = 10$; $P = 0.25$) or RIT alone (20%; $n = 10$; $P = 0.25$). In addition, NFV/RIT, when given 4 hours after SEB/D-gal, was associated with improved survival compared with control (60%; $n = 10$; $P < 0.05$; Figure 1C). NFV/RIT treatment was also associated with reduced V-β8 T cell apoptosis compared with vehicle control (Figure 1D).

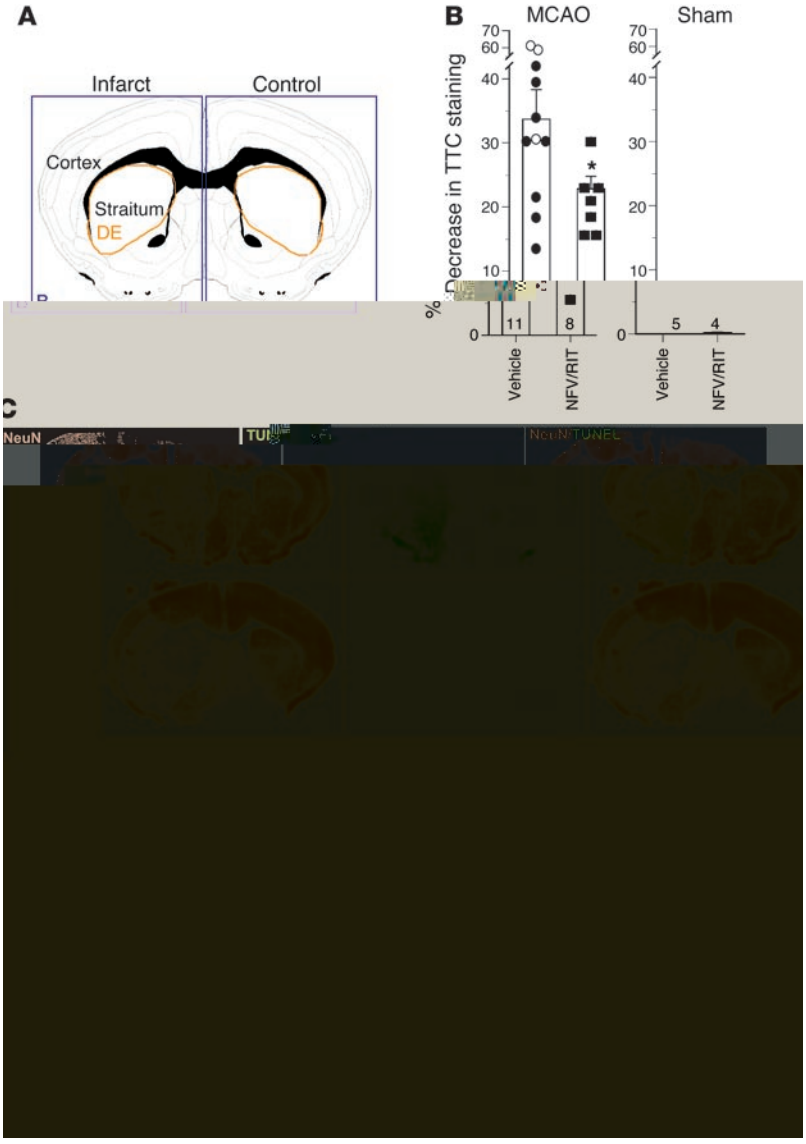

Figure 2
Effects of NFV/RIT on infarct size, neuronal loss, and behavioral impairment following 1 hour of MCAO and 24 hours of reperfusion. (**A**) Schematic representation of coronal forebrain sections were analyzed. Infarcted and control hemispheres are indicated. DE, diencephalon. The tissue areas analyzed by TTC as shown in **B** are indicated in blue. The areas analyzed for NeuN and TUNEL reactivity as shown in **D** and **E** are indicated in orange. (**B**) Mice pretreated with NFV/RIT exhibit a smaller infarct 24 hours after surgery, as assessed by TTC staining, relative to mice pretreated with vehicle or control (sham) mice (*P < 0.05, Student's t test). Open circles, no pretreatment; filled circles, vehicle pretreatment; filled squares, NFV/RIT pretreatment. (**C**) NFV/RIT protects neurons from apoptotic-like death. (**D**) Quantitation of overall neuronal loss following MCAO or sham surgery. Both vehicle- and NFV/RIT-treated animals exhibit a comparable reduction in neuronal number following MCAO (#P = 0.08, *P < 0.05, ANOVA, post-hoc Dunnett t test). (**E**) NFV/RIT-treated animals are protected from apoptotic-like death following MCAO surgery. The majority of remaining NeuN-positive cells in vehicle-treated mice are apoptotic, while TUNEL reactivity is significantly reduced in NFV/RIT-treated animals (**P < 0.01, ANOVA, post-hoc Dunnett t test). (**F**) NFV/RIT improves neurological recovery following MCAO. Animals tested immediately after MCAO surgery (0.5 hours) show equivalent motor deficits. After 24 hours of reperfusion, NFV/RIT exhibit significant behavioral improvement relative to 0.5 hours or vehicle-treated cells. *P < 0.05; **P < 0.01, ANOVA, post-hoc Tukey test. Data represent mean ± SEM.

Given the substantial reduction in apoptosis and the improvement in survival afforded b NFV/RIT in the Jo-2 and SEB models, we ne t assessed the impact of NFV/RIT on cerebral injur in the middle cerebral arter occlusion (MCAO) model of focal ischemia. C57BL/6 mice were pretreated b oral gavage with either NFV/RIT or vehicle (2% EtOH) 24, 16, and 8 hours before sham or MCAO surger (vehicle control, sham surger , n = 7; vehicle control, MCAO, n = 10; NFV/RIT, sham surger , n = 7; NFV/RIT, MCAO surger , n = 10). A fifth cohort received MCAO surger without NFV/RIT or vehicle pretreatment (n = 5). Infarct si e in the striatum and corte was assessed b 2,3,5-triphen ltetra olium (TTC) staining (Figure 2A). After 1 hour of MCAO followed b 24 hours of reperfusion, vehicle-treated animals or mice that were not orall gavaged e hibited a 34% reduction in TTC staining (Figure 2B). Infarct si e as measured b TTC staining was 23% (P < 0.05 compared with control) in the NFV/RIT treatment group (Figure 2B). We ne t assessed neuronal number in the striatum b immunodetection of the neuron-specific marker NeuN (24). Both vehicle- and NFV/RIT-treated animals e hibited a comparable, appro imatel 20% loss of NeuN-positive neurons after 1 hour of MCAO and 24 hours of reperfusion (Figure 2, C and D). However, NFV/RIT significantl reduced apoptotic-like death, as detected b TUNEL/NeuN double labeling (Figure 2, C and E). In vehicle-treated animals, 67% of the remaining NeuN-positive neurons in the striatum were activel undergoing DNA fragmentation 24 hours after surger (Figure 2, C and E); however, onl 24% (P < 0.01) of NeuN-positive neurons were TUNEL reactive in NFV/RIT-treated mice (Figure 2, C and E). Finall , we determined whether the neuroprotection afforded b NFV/RIT pretreatment manifested in improved behavioral recover . Neurological deficits in motor function were assessed using an e panded 6-point scale modified from refs. 25, 26 (see Methods). Animals were tested immediatel after 0.5 hours of MCAO and again 24 hours after reperfusion. NFV/RIT-pretreated animals e hibited comparable motor deficits after 1 hour of MCAO compared with vehicle-treated or control animals (no pretreatments) but evident behavioral improvement 24 hours after surger (Figure 2F), consistent with the reduction in apoptotic loss and reduced infarct si e.

To anal e the antiapoptotic mechanism of NFV/RIT in vivo, we compared apoptotic signaling in Jurkat T cells stimulated in

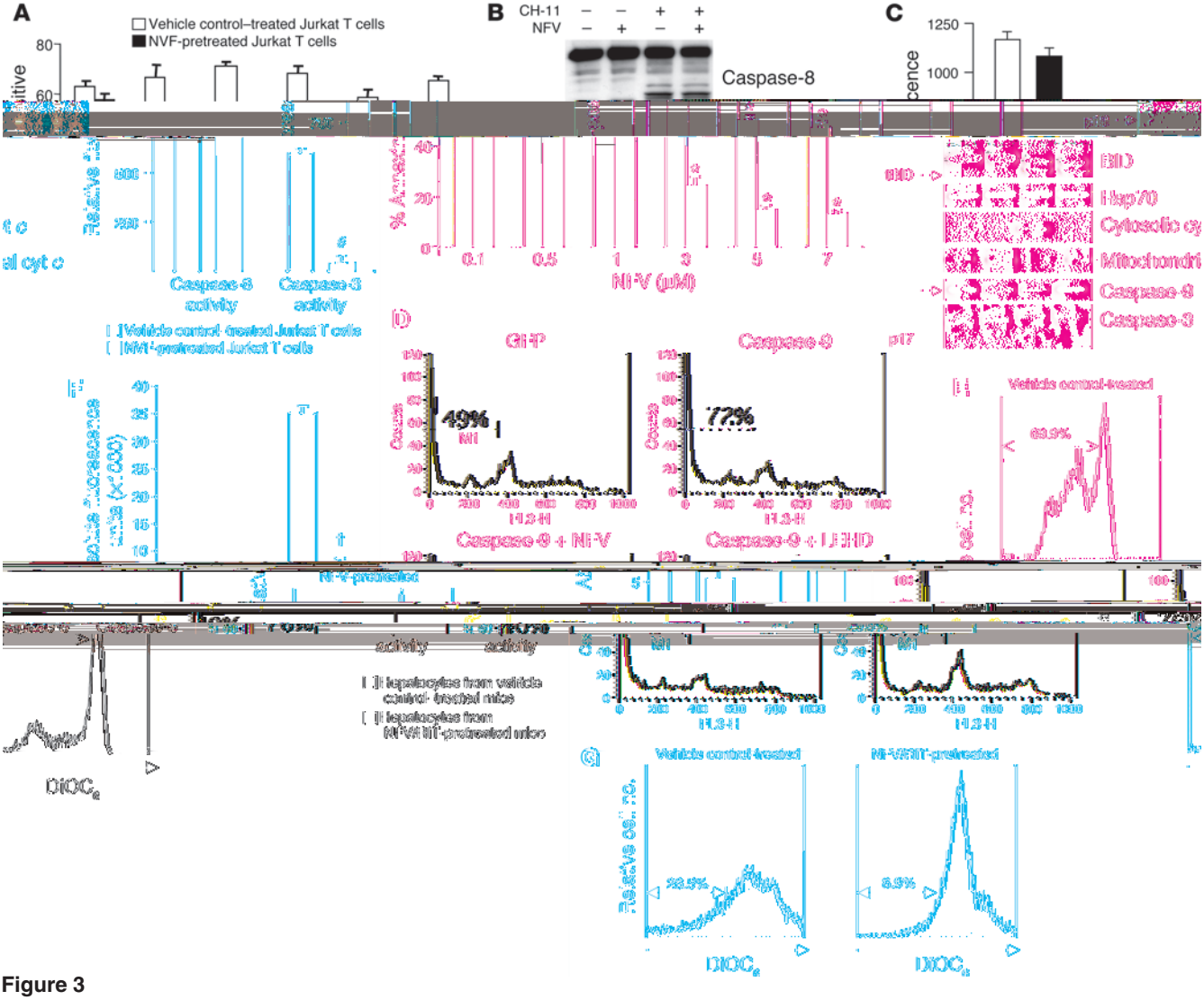

Figure 3

Effect of NFV on apoptotic signaling events in vitro and in vivo. (**A**) Jurkat T cells were stimulated with agonistic anti-Fas antibody (CH-11) in the presence or absence of varying concentrations of PI and analyzed for annexin positivity. $^{*}P < 0.05$. (**B**) Western blot analysis of the Fas signaling events of caspase-8, -9, and -3 cleavage, BID cleavage, or cytosolic translocation of cytochrome *c* (cyt *c*) in Jurkat T cells treated or not treated with CH-11 with or without NFV. tBID, truncated BID. (**C**) Caspase-8 and caspase-3 activity was also assessed in Jurkat T cells stimulated with CH-11 in the presence or absence of NFV. $^{\#}P < 0.01$. (**D**) Jurkat cells were transiently transfected by a GFP plasmid or a caspase-9 GFP plasmid, treated or not treated with 7 μM NFV or 100 μM LEHD, cultured for 6 hours, stained with PI, and analyzed by cytofluorometry for hypoploidy. (**E**) Jurkat cells stimulated with CH-11 in the presence or absence of NFV were analyzed for loss of $DiOC_6$ retention. Hepatocytes isolated from mice receiving Jo-2 with NFV/RIT or control (as in Figure 1) were also analyzed for caspase-8 and caspase-3 activity (**F**) and loss of $DiOC_6$ retention (**G**). $^{\dagger}P < 0.005$.

vitro with CH-11 anti-Fas antibod with the apoptotic signaling in hepatoc tes isolated from mice treated in vivo with IV Jo-2 anti-Fas antibod . In vitro pretreatment of Jurkat T cells with NFV followed b stimulation with CH-11 resulted in a dose-dependent reduction in apoptosis (Figure 3A). NFV-pretreated Jurkat T cells had similar caspase-8 cleavage and activit and Bid cleavage as seen in vehicle control cells. However, mitochondrial membrane permeabilit ($\Delta\Psi_m$), c tochrome *c* release, caspase-9 cleavage, and caspase-3 cleavage and activit were all reduced b NFV pretreatment (Figure 3, B, E), which suggests that NFV inhibition of apoptosis occurs upstream of caspase-9 in the apoptotic pathwa . Moreover, transient e pression of caspase-9 in Jurkat T cells resulted in h poploid that was not inhibited b NFV et was inhibited b the caspase-9 inhibitor, LEHD, which confirms that NFV blocks apoptosis upstream of caspase-9 activation. Similar anal ses were performed e vivo on hepatoc tes isolated from mice pretreated with either NFV/RIT or vehicle control and subsequentl challenged with IV Jo-2. In these cells, caspase-8 activation was unaltered b NFV/RIT pretreatment, whereas caspase-3 activit was significantl ($P < 0.005$) inhibited (Figure 3F). Additionall , loss of $\Delta\Psi_m$ was evident in vehicle control hepatoc tes but was blocked in the hepatoc tes of mice that received NFV/RIT pretreatment (Figure 3G). Therefore, in vitro and in vivo, PIs inhibit mitochondrial $\Delta\Psi_m$ and subsequent postmitochondrial signaling events.

To confirm that the effect of NFV locali es to mitochondria, we treated isolated mitochondria with Vpr, atract loside (ATR), Ba

and determined that NFV inhibits mitochondrial swelling induced b all 3 stimuli (Figure 4A). Inhibition of Ba -induced apoptosis might indicate a loss of Ba activation and translocation or a lack of effect of Ba on $\Delta\Psi_m$ (reviewed in refs. 27, 28). We therefore directl assessed whether NFV inhibited mitochondrial translocation and activation of Ba . We stimulated cells through the Fas receptor in the presence of NFV or DMSO vehicle control and anal ed them for nuclear morpholog using Hoechst 33342 staining and for Ba activation b immunofluorescence using an antibod specific for the activated conformation of Ba . Control (untreated) cells had no evidence of Ba activation and had intact nuclei. Fas-stimulated cells e hibited both Ba activation with punctate Ba staining and fragmented nuclei, consistent with apoptosis. NFV-pretreated cells showed punctate staining for activated Ba , et no nuclear fragmentation was observed (Figure 4B).

Furthermore, we induced apoptosis b overe pression of Ba . Ba was cotransfected with GFP, and consequentl apoptosis was assessed specificall in the GFP-positive cell populations. NFV treatment inhibited $\Delta\Psi_m$ loss induced b the overe pression of Ba (Figure 4C). Together, therefore, our data indicate that the antiapoptotic action of NFV occurs at the level of mitochondria, downstream of Ba translocation and activation, but invoking mitochondrial $\Delta\Psi_m$.

Mitochondrial loss of $\Delta\Psi_m$ is coincident with the opening of the mitochondrial permeabilit transition pore comple (PTPC). These events allow the release of c tochrome *c* into the c tosolic compartment, which, in the presence of dATP, results in the formation of a comple between Apaf-1 and procaspase-9 known as the apoptosome. This results in activation of procaspase-9 (29, 30), which in turn activates the downstream effector caspase-3 (31). A ke regulator in this process, therefore, is the mitochondrial PTPC, which is composed of the peripheral ben o-dia epine receptor (PBR), adenine nucleotide translocator (ANT), voltage-dependent anion channel (VDAC), as well as other proteins (32). We therefore assessed apoptosis in the presence or absence of NFV in WT east or east deficient in both isoforms of VDAC or all 3 isoforms of ANT. HIV Vpr initiates apoptosis through binding ANT with affinities in the nanomolar range (33), whereas Vpr does not bind to VDAC in vitro (33). Consistent with prior reports, Vpr was able to induce east death onl if ANT was present (Figure 5, A and B). Since VDAC and ANT ph sicall interact, and form the principal pore channel of PTPC in a cooperative manner (34, 35), absence of VDAC also abrogated the abilit of Vpr to cause death (Figure 5A). H_2O_2 also induces apoptosis in an ANT-dependent manner, potentiall through o idation of thiol groups within ANT (36, 38). Like Vpr, H_2O_2 onl induced apoptosis if ANT was present, and VDAC was required as well (Figure 5A). Ne t, we assessed the abilit of NFV to inhibit apoptosis in WT east following stimulation with Vpr or H_2O_2. WT east underwent Vpr- and H_2O_2-induced apoptosis, which was inhibited in a dose-dependent manner b NFV treatment (Figure 5B), arguing that NFV requires the presence of ANT, VDAC, or both.

To further e amine the involvement of the components of the PTPC in NFV-mediated inhibition of apoptosis, we ne t used chemical ligands that selectivel interact with different components of the PTPC, causing it to open and resulting in subsequent loss of $\Delta\Psi_m$. PK11195 is an agonist of the PBR (39, 40), ATR is an agonist of ANT (41), and staurosporine (STS) is an agonist of VDAC (42, 43). Jurkat T cells were pretreated with NFV or vehicle control and subsequentl treated with these agonists and anal ed for apoptosis. Treatment with PK11195 or STS resulted in apoptosis (Figure 6A), loss of $\Delta\Psi_m$ (Figure 6B), c tochrome *c* release, caspase-9 cleavage, caspase-3 cleavage and activation, and pol (ADP-ribose) pol merase (PARP) cleavage (Figure 6, C and D) that were not altered b NFV, which suggests that NFV does not alter PBR or VDAC-initiated loss of $\Delta\Psi_m$. Repeating these e periments with the ANT-specific agonist ATR resulted in a loss of $\Delta\Psi_m$, c tochrome *c* release, caspase-9 cleavage, caspase-3 cleavage, PARP cleavage, and caspase-3 activation that were inhibited b NFV (Figure 6, A, D). These differential results suggest that NFV acts as an inhibitor of ANT-dependent PTPC opening.

To confirm that NFV can act specificall with ANT to inhibit its pore function, we used proteoliposomes reconstituted with either entire PTPC or with ANT alone, which release a fluorescent d e following pore opening (44). Consistent with our cellular data, treatment of PTPC liposomes with ATR results in significant fluorescence release that was progressivel inhibited b a range (0.1, 10 μm) of increasing doses of NFV (Figure 7A). We

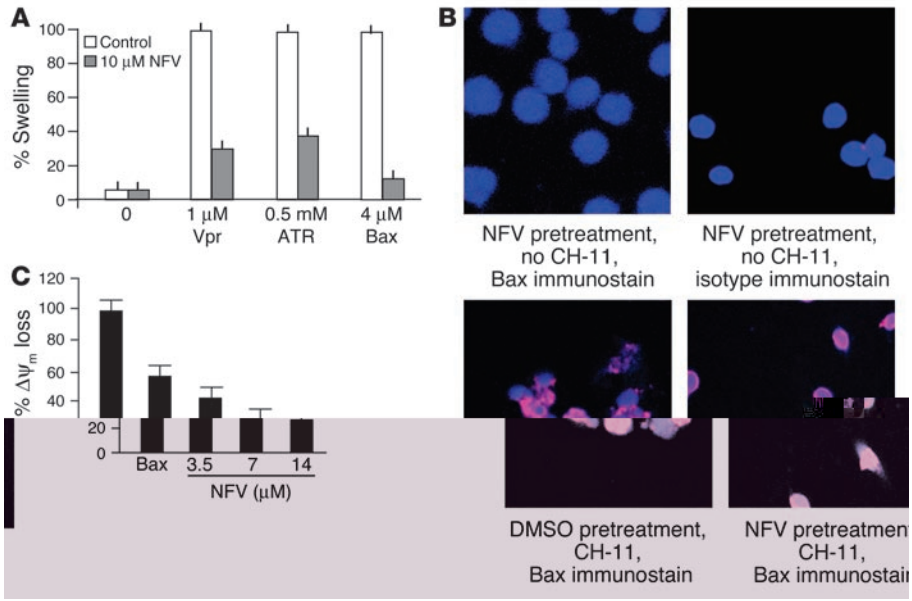

Figure 4
NFV blocks Bax-induced apoptosis but not Bax activation. (**A**) Mouse liver mitochondria were incubated with 10 μM of NFV followed by 1 μM Vpr-derived peptide, 0.5 mM ATR, or 4 μM Bax while absorption was assessed at 545 nm. The loss of absorption induced by 0.5 mM ATR within 20 minutes was considered at 100% of large amplitude swelling. All experiments were reproduced 3 times. (**B**) Jurkat T cells were treated with an agonistic anti-Fas antibody in the presence or absence of NFV and stained with Hoechst 33342 for nuclear morphology, an antibody (or isotype control) specific for activated Bax, and an Alexa Fluor–conjugated secondary antibody. All cells were stained with Hoechst and varying combinations of NFV or DMSO, CH-11, and anti-Bax or isotype antibody as indicated. (**C**) Jurkat T cells were transfected with Bax, and immediately following transfection, NFV or control was added and $\Delta\Psi_m$ was assessed.

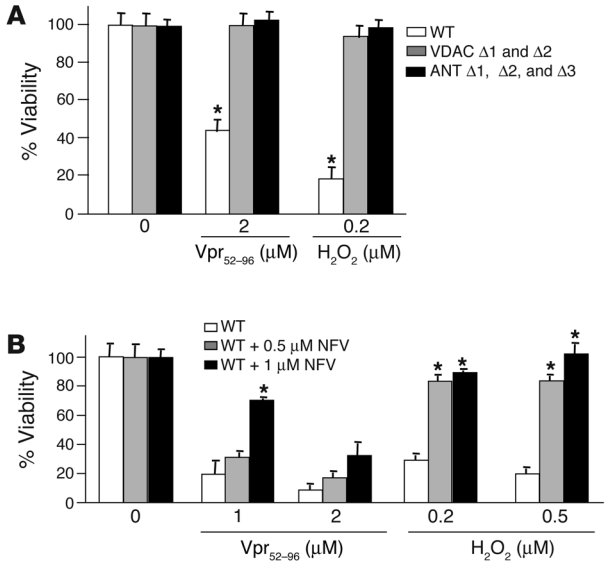

Figure 5
Effects of NFV on apoptosis in yeast. (**A**) WT yeast or yeast deficient in both isoforms of VDAC (VDAC Δ1 and Δ2) or 3 isoforms of ANT (ANT Δ1, Δ2, and Δ3) were treated with the apoptosis-inducing agents Vpr peptide (residues 52–96) or H_2O_2 and analyzed for viability. (**B**) WT yeast treated with varying doses of NFV was treated with the same apoptosis inducers and analyzed for viability. Results are representative of 3 independent experiments. *$P < 0.05$.

ne t assessed whether NFV could act directl upon ANT to inhibit its pore function. ANT liposomes were created and treated with 2 distinct ANT ligands, ATR (Figure 7B) and Vpr (Figure 7C). Each ligand resulted in a dose-dependent release of fluorescence from the ANT liposomes that in turn was inhibited ($P < 0.05$) in a dose-responsive manner b NFV.

Discussion

Here we provide evidence that HIV PIs have the abilit to meaningfull impact apoptosis in vivo in a variet of animal models and that this effect locali es to mitochondrial release of proapoptotic factors. Moreover, our in vitro data suggest that NFV acts to inhibit the pore function of the ANT subunit of the mitochondrial PTPC. This effect of NFV permits the premitochondrial signaling events of death receptor initiated apoptosis et inhibits mitochondrial loss of $\Delta\Psi_m$ and the subsequent formation of the apoptosome and activation of caspase-9 and caspase-3.

This mechanism of action offers insight into the question of whether cells that have undergone some changes of apoptosis (e.g., caspase-8 activation) but not others (e.g., $\Delta\Psi_m$) will still be fated to death. Hepatoc tes from Jo-2 treated mice dosed with NFV/RIT maintained caspase-8 activation but not the mitochondrial and postmitochondrial signaling events. Consequentl , anal sis of these mice affords an opportunit to address the long-term outcome of tissues rescued from death b NFV/RIT treatment. First, since no mortalit was observed between da s 3 and 30, NFV/RIT treatment prevents rather than dela s death. Second, serum AST remains lower in NFV/RIT-treated mice, which suggests maintenance of hepatoc te viabilit and function. Third, hepatic histolog of NFV/RIT-treated mice is preserved at da 30, which demonstrates a lack of dela ed tissue damage in mice surviving as a consequence of NFV/RIT therap . Comparable results were

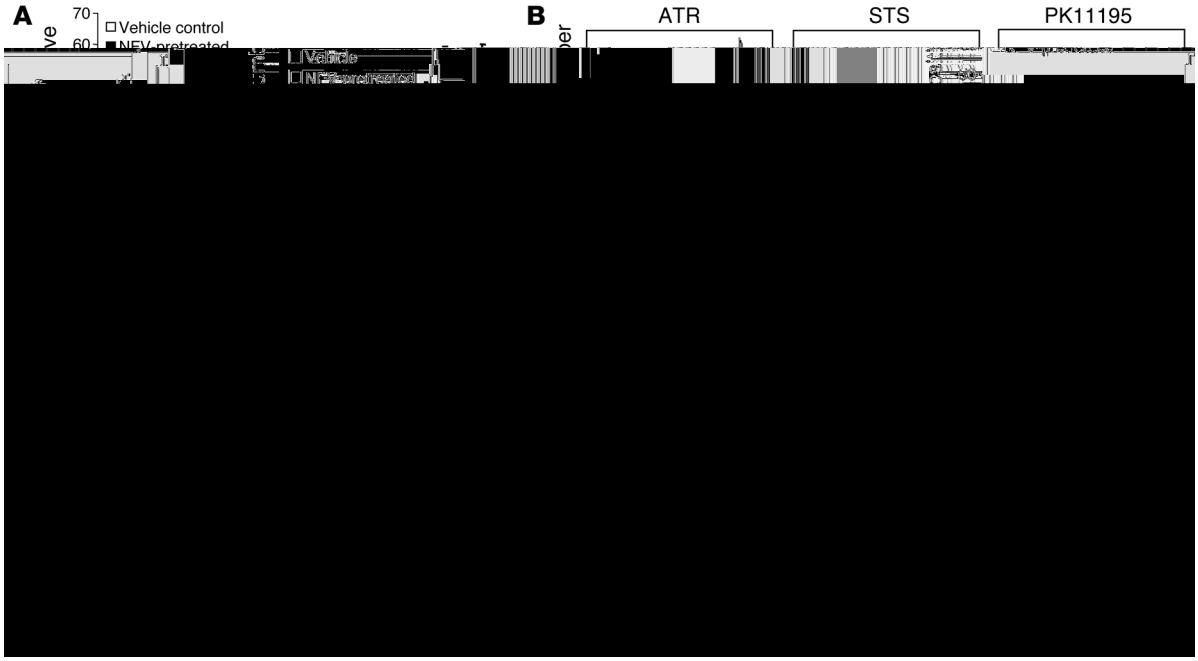

Figure 6
Effects of NFV on the apoptosis-inducing abilities of the selective PTPC agonists. Jurkat T cells were treated with either the ANT agonist ATR, VDAC agonist STS, or PBR agonist PK11195, in the presence or absence of PI, and analyzed for annexin positivity (**A**), loss of $DiOC_6$ retention (**B**) caspase-9, caspase-3, and poly (ADP-ribose) polymerase (PARP) cleavage and cytosolic release of cytochrome *c* (**C**), and caspase-8 and caspase-3 activity (**D**). Results are representative of 3 independent experiments. *$P < 0.01$.

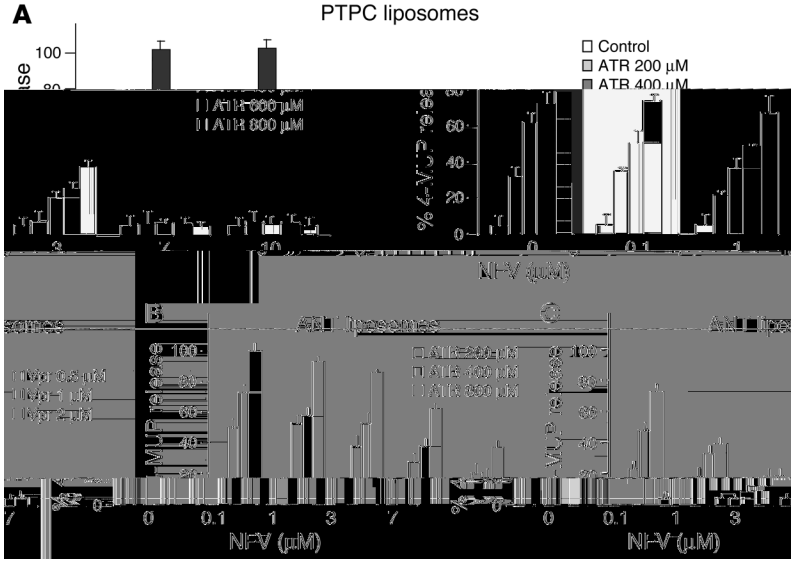

Figure 7
Effects of NFV on PTPC or ANT pore function. (**A**) Proteoliposomes containing PTPC complexes were treated with NFV, stimulated with ATR, and analyzed for fluorescence release. Proteoliposomes containing ANT were treated with NFV and analyzed for fluorescence release following stimulation with ATR (**B**) or Vpr peptide (residues 52–96) (**C**). Results are representative of 3 independent experiments.

observed in the MCAO model of focal ischemia. NFV/RIT did not affect necrotic loss or neuronal damage in the ischemic core, nor did pretreatment improve behavioral indices when animals were tested after recover from the anesthetic, 30 minutes after the 1-hour occlusion. However, NFV/RIT significantl reduced subsequent apoptotic-like death observed over the 24-hour reperfusion period, markedl improving neurological scores as a consequence. Therefore, blocking the mitochondrial events of apoptosis represents a viable approach to preventing rather than dela ing cell death and a potential means of improving function in pathologic processes involving e aggerated apoptosis.

It is noteworth that the antiapoptotic effects of NFV/RIT persist even if administered after the apoptosis-initiating event in mice receiving SEB/D-gal, and survival is improved when NFT/RIT is administered 4 hours later. Although the ma imum duration between apoptotic insult and NFV/RIT administration that is still associated with improved outcome remains to be defined, these observations suggest the increased likelihood that such agents might afford clinicall useful protection.

Recentl , the role of ANT in mitochondrial permeabilit transition has been questioned. Whereas ANT has been widel regarded as being essential for mitochondrial depolari ation and consequent c tochrome *c* release, apoptosome formation, and apoptosis, a recent report directl challenges that role. Mice were constructed with a complete deficienc in both isoforms of ANT within liver tissues (45). Hepatoc tes from these mice had compensator upregulation of c tochrome *c* and of c tochrome *c* o idase. Mitochondria from these livers contain functional PTPCs, which release c tochrome *c*; however, 3-fold more calcium signal was required to induce the permeabilit transition than in WT cells. Thus, although the knockout of ANT-1 and ANT-2 genes in hepatoc tes does not abolish mitochondrial outer membrane permeabili ation induced b calcium in absolute terms, it does significantl reduce the sensitivit of these mitochondria to calcium-induced PTPC opening. Our current data are consistent with some findings discussed in that report; both inhibition of ANT b PIs and genetic absence of ANT result in abrogated mitochondrial response to ANT ligands, including ATR. However, unlike cells from ANT-deficient livers, which remain sensitive to apoptosis induced b Fas ligand and TNF-α, PI-treated cells acquire resistance to Fas signaling. It is not clear to what e tent adaptive responses involving e pression of other mitochondrial carrier proteins (which might assume the functions of ANT) ma compensate for the defect in ANT-1 and ANT-2, at either the bioenergetic level or the cell death regulator level (46). B no means do the data from the knockout model e clude the possibilit that pharmacologic apoptosis modulation can be achieved through inhibition of ANT function.

E amining the -ra cr stal structure of ANT, we studied whether NFV can be predicted to interact with ANT. Computer simulations of the interactions of NFV with ANT indicated a putative binding site on the matri side of the transporter protein. Based on this simulation, NFV is predicted to bind close to helices 3 and 5 of ANT (Figure 8). Binding also involves part of the loop connecting helices 3 and 4 (loop M2 in Figure 8), which has been proposed as the ADP binding site (37). Several h drogen bonds appear to be made between NFV and ANT, in particular with residues K162, G242 (backbone), M239 (backbone), and R243 (Figure 8). H drophobic contacts between NFV and ANT constitute the segment around S166 as well as the side chain of R139.

Since multiple apoptotic signals, including death receptor ligation, chemotherapeutics, BH3-onl Bcl2 famil members, UV radiation, and others converge upon mitochondria, drugs that target mitochondrial regulators of apoptosis, such as NFV, are attractive therapeutic candidates. Our data provide the basis for the evaluation of NFV or related compounds as in vivo inhibitors of apoptosis in non-HIV disease states characteri ed b e cessive apoptosis.

Methods

Mouse treatments

Mice received either NFV/RIT in 2% ethanol or vehicle control (2% ethanol) b oral gavage ever 8 hours. Animal treatments were reviewed and approved b the Ma o Foundation Institutional Animal Care and Use Committee, the NRC/IBS Animal Care Committee, and the Universit of Ottawa Animal Care Committee. Plasma concentrations of NFV and RIT were measured simultaneousl using liquid chromatograph with tandem mass spectrometr . The lower limit of quantitation for NFV and RIT was 2.5 ng/ml. The accurac of qualit control samples anal ed simultaneousl with the stud samples ranged from 83.7% to 107.5% for NFV and 105.0% to 116.5% for RIT. The within-run variabilit for 3 replicative anal ses of the qualit control samples was less than 9.7% for both NFV and RIT. This assa has been cross-validated as part of the International Interlaborator Qualit Control Program for Therapeutic Drug Monitoring in HIV Infection (47). To determine a dosing regimen that would result in relevant plasma concentrations, we treated 6- to 8-week-old BALB/c and C57BL/6 mice with 250 mg/kg of NFV (Agouron Pharmaceuticals Inc.) ever 8 hours, et plasma concentrations were undetectable 6 hours after dosing. Since coadministration of RIT in humans significantl increases

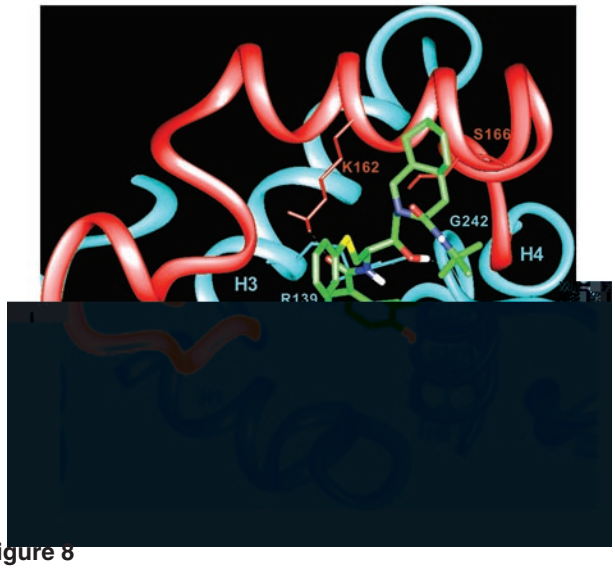

Figure 8
Computer-simulated model of NFV interaction with ANT. Close-up of the proposed binding mode of NFV to the matrix side of ANT. Parts of helices 1, 3, 4, and 5 (H1, H3, H4, and H5) are shown. Loop M2, connecting helices 3 and 4, is shown in red. Hydrogen bonds are displayed as dotted lines. Side chains or backbone atoms of selected residues are shown (see Methods). The PI is colored according to atom types: C, green; O, red; N, blue; S, yellow.

NFV levels compared with NFV alone (48), we treated mice ever 8 hours with 125 mg/kg NFV and 13 mg/kg RIT (Abbott Laboratories). Eight-hour NFV trough levels, ranging from 1,199 to 1,258 ng/ml, were comparable to concentrations observed in HIV-infected patients using NFV. We also assessed whether C57BL/6 mice treated with this dose of NFV/RIT achieved detectable drug levels in the brain. NFV and RIT concentrations in brain tissues were determined after the tissues were washed e tensivel with PBS, blotted dr with filter paper, placed in 5 ml of 0.1 M phosphoric acid, and homogeni ed using a pol tron. Supernatants were anal ed as described above for drug level determination. Anal sis of whole brains revealed levels of NFV between 682 and 986 μg/g of brain tissue. We therefore opted to assess the in vivo antiapoptotic effects of the combination of NFV and RIT using this dosing regimen.

Fas-induced liver failure

Si -week-old female C57BL/6 mice (Charles River Laboratories) received the indicated doses of Jo-2 anti-Fas antibod (BD Biosciences Pharmingen) b tail vein injection. Moribund animals, or animals who survived until the indicated time points, were sacrificed b CO_2 asph iation. Clinical chemistries were performed on serum obtained from 3 mice from each treatment group at 4 and 24 hours after Jo-2 injection. Quantitation of hepatoc te apoptosis b TUNEL assa (Roche Diagnostics Corp.) was averaged from results anal ses performed in a blinded manner b 4 reviewers.

SEB-induced shock

Si -week-old female BALB/c mice (Harlan) received 20 mg D-gal (Sigma-Aldrich) and 6.5 μg SEB (To in Technolog Inc.) intraperitoneall . Animals were euthani ed if the became moribund, laterall recumbent, or h pothermic (rectal temperature <32 C) at the indicated time points. Spleens were harvested and splenoc tes isolated mechanicall with plastic mesh. Following red cell l sis and removal of B cells b incubation with n lon wool (1 hour, 37 C; Accurate Chemical and Scientific Corp.), purified T cells were stained with monoclonal anti-mouse V-β8, FITC antibod (clone F23.1), V-β3, FITC antibod (Clone KJ25), or appropriate isot pe control (BD Biosciences Pharmingen) and then washed with PBS and fi ed with 1% paraformaldeh de. Dual staining with TUNEL-TMR red (Roche Diagnostics Corp.) was performed as per the manufacturer's instructions.

Cerebral ischemia produced by MCAO

C57BL/6 mice (20, 23 g) were obtained from Charles River Laboratories. Under temporar isofluorane anesthesia, mice were subjected mice to MCAO using an intraluminal filament as previousl described (49). After 1 hour of MCAO, the filament was withdrawn, blood flow restored to normal b laser Doppler flowmetr , and wounds sutured. Beginning 24 hours before surger , mice received 3 oral gavages, 8 hours apart, of either NFV/RIT or vehicle. Following 24 hours of reperfusion, mice were anestheti ed with CO_2 and sacrificed b either decapitation or lethal injection with sodium pentobarbital and transcardiall perfused with 10 mM PBS (10 mM sodium phosphate and 154 mM NaCl) followed b 3.7% paraformaldeh de in 10 mM PBS. Behavioral impairment following MCAO was assessed at 30 minutes after ischemic surger when animals had recovered from the anesthetic and 24 hours after reperfusion b 2 investigators blind to the treatment of the mice. A modified 6-point scale was used (25, 26): 0, normal; 1, mild turning behavior with or without inconsistent curling when picked up b tail and less than 50% attempts to curl to the contralateral side; 2, mild, consistent curling and more than 50% attempts to curl to the contralateral side; 3, strong and immediate consistent curling, mouse holds curled position for more than 1, 2 seconds, and mouse's nose almost reaches tail; 4, severe curling progressing into barreling and loss of walking or righting refle ; 5, comatose or moribund. Behavioral scores were averaged within treatment groups for statistical anal sis. In unfi ed tissue, infarct si e was measured b a colorimetric staining method using TTC, as described previousl (50). Brains were removed and cut into three 2-mm-thick coronal slices through forebrain, which were separated into left and right hemispheres and stained with 5 ml of 2% TTC per hemisphere for 90 minutes at 37 C. The tissue was rinsed with saline, and the forma an product solubili ed in ethanol/DMSO (1:1). After a 24-hour incubation in the dark, the red solvent e tracts were diluted 1:20 with fresh ethanol/DMSO solvent in triplicate, absorbance was measured at 485 nm in a spectrophotometer, and the values were averaged. Percent decrease in brain TTC staining was calculated using the following equation: percent decrease = [100, (absorbance of contralateral hemisphere/absorbance of ischemic hemisphere) × 100]; and the values for the ischemic and contralateral sides of the brain in the same animal were compared. Perfused brains were postfi ed for 24 hours in 3.7% paraformaldeh de in 10 mM PBS and cr oprotected in 20% sucrose solution in 10 mM PBS containing 0.001% sodium a ide. Serial coronal sections (10 μm) were cr ostat cut (Leica Micros stems Inc.). Neuronal apoptosis was confirmed in fi ed tissue b reaction for TUNEL (Roche Diagnostics Corp.) and immunolabeling for the neuronal nuclear marker NeuN (Chemicon International) using a C 3-conjugated anti-mouse IgG secondar antibod (Jackson ImmuoResearch Laboratories Inc.) as described (51). Antibodies were diluted in antibod buffer (10 mM PBS, 0.3% Triton X-100, and 3% BSA). We evaluated immunofluorescence using on a DMRXA2 microscope (Leica Micros stems Inc.) equipped for epifluorescence. The number of NeuN-positive/TUNEL-negative cells was counted and tissue area was measured using the Advanced Measurements Module of OpenLab version 3.17 (Improvision) in 2 adjacent sections of both ipsilateral and contralateral striatum and corte . Means were averaged across treatment groups.

Cell culture and apoptosis induction in vitro

Jurkat T cells (ATCC) were cultured in RPMI media (Mediatech Inc.), supplemented with 10% heat-inactivated FBS (Atlanta Biologicals), and peni-

cillin/streptom cin (Invitrogen Corp.) at 37 C in 5% CO_2. Where indicated, cells were incubated with 7 μM NFV or 20 μM -VAD-fmk (R&D S stems) or vehicle (DMSO) overnight prior to induction of apoptosis with indicated doses of CH-11 anti-Fas antibod (Upstate), ATR (Sigma-Aldrich), STS (Calbiochem), or PK11195 (Sigma-Aldrich).

Transfection experiments

Transient transfection of Jurkat cells with vectors containing a pEGFP gene (pEGFP-N2; BD Biosciences), a Ba -GFP gene (kindl provided b Shigemi Matsu ama, Research Center for Allerg and Immunolog , Kanagawa, Japan; ref. 52), and caspase-9 GFP (kindl provided b P. Mehlen, Apoptosis Cancer and Development Laborator , L on, France; ref. 53). Cells were cultured in RPMI 1640, 10% FBS, and 1% L-glutamine without antibiotics. Two da s before transfection, cells were passed at 1.5×10^5 cells/ml. For electroporation, 1×10^7 cells were pelleted, resuspended in 250 μl of 10% FBS-RPMI 1640, mi ed with 250 μl of 20 μg DNA, and incubated for 10 minutes at room temperature (RT). The DNA/cell suspension was transferred to a 4-mm cuvette, and electroporation was performed at 10 ms/325 V using a square wave electroporator (Bio-Rad Laboratories). After 10 minutes at RT, cells were diluted to 20 ml in complete medium without antibiotics and cultured at 37 C under 5% CO_2. NVF, DEVD (Bachem), and LEHD (Bachem) were added following electroporation (54).

Hepatocyte isolation

Four hours after treatment with 7.5 μg of Jo-2 antibod , mice were euthani ed with pentobarbital (60 mg/kg; Abbott Laboratories) and hepatoc tes isolated via a 2-step collagenase digestion (55). Following red cell l sis, hepatoc tes were enumerated and evaluated for apoptosis through loss of $\Delta\Psi_m$ and caspase-8 and caspase-3 activit .

Assays of apoptotic signaling: TUNEL

Briefl , 1×10^6 cells were fi ed with 2% paraformaldeh de, permeabili ed with 0.1% Triton X-100 and 0.1% citrate, and stained with TUNEL as per the manufacturer's directions (Roche Diagnostics Corp.).

DNA content

For cell c cle anal sis, cells (5×10^5/ml) were spun down and fi ed in 70% ice-cold ethanol/PBS, added dropwise while vorte ing, kept at 20 C, and centrifuged. Cells were resuspended in 1 ml PBS containing RNAse and 50 μg/ml propidium iodide (Invitrogen Corp.) and anal ed in a c tofluorometer (56).

Annexin V and propidium iodide staining. Fift microliters of anne in binding buffer (BD Pharmingen) was added to 1×10^6 cells in 500 μl of media followed b 2 μl of anne in V FITC (BD Pharmingen) and 1 μl of propidium iodide (Sigma-Aldrich). The mi ture was vorte ed and incubated for 30 minutes at 37 C and then subjected to FACS anal sis.

Western blot analysis. We subjected 40 60 μg of protein from whole cell l sates to SDS-PAGE. Following transfer, PVDF membranes (Millipore) were probed with antibodies to caspase-3 (1 μg/ml; Gene Therap S stems Inc.), caspase-9 (1 μg/ml; Medical & Biological Laboratories Co.), c tochrome *c* (1 μg/ml; BD Biosciences Pharmingen), or PARP (1 μg/ml; BD Biosciences Pharmingen). Following incubation with goat anti-mouse HRP (1:10,000; Amersham Biosciences), an enhanced chemiluminescence assa (Amersham Biosciences) was used to detect the proteins of interest. Where indicated, mitochondria were separated from c tosols for subcellular detection of c tochrome *c*, as previousl described (57). Briefl , cell l sates were harvested and centrifuged twice at 15,000 *g* (4 C) for 15 minutes to fractionate the c tosolic (supernatant) fraction from the mitochondrial pellet. Aliquots of c tosolic or mitochondrial protein (200 μg) were separated b 4 15% gradient SDS-PAGE and probed with monoclonal antibod against c tochrome *c*.

Fluorometric caspase-8 and caspase-3 activity. We resuspended 150-μg aliquots of whole cell l sates in reaction buffer with the appropriate fluorogenic caspase substrate (IETD for caspase-8 and DEVD for caspase-3) (R&D S stems). Activit was determined with a fluorescence plate reader (BIOTEK Inc.) at an e citation wavelength of 400 nm and emission of 505 nm.

$DiOC_6$ staining. We incubated 1×10^6 intact cells with 40 nM $DiOC_6$ (Invitrogen Corp.) for 30 minutes at 37 C prior to FACS anal sis.

Mitochondrial swelling

Mitochondria were purified from BALB/c mouse livers on a Percoll gradient (58) and were stored on ice for up to 4 hours. For determination of large amplitude swelling, 5 μl of mitochondria (0.5 mg protein/ml) was added to 200 μl of swelling buffer [0.2 M saccharose, 10 mM TRIS-3-(N-morpholino) propanesulfonic acid, 5 mM propidium iodide, 1 mM EGTA, 0.35 mM rotenone, pH 7.4], and light absorption was recorded for 20 minutes at 545 nm in a microtiter plate (TECAN GENios). The loss of absorption induced b 0.5 mM ATR was used as a positive control to define ma imal large amplitude swelling. For inhibition e periments, NFV or control was alwa s added before the swelling inducers, Vpr-derived peptide, and ATR.

Yeast strains and clonogenic assays

We pretreated 10^4 cells/ml of *Saccharomyces cerevisiae* M 22-2-1 (genot pe *MATa ade2 leu2 lys2 his4 trpl ura3 Canr, por1:LEU2, por2:TRP1*; gift from M. Forte, Vollum Institute, Portland, Oregon, USA) (59, 60), *S. cerevisiae* W301-1B control strain (*MATa ade2, leu2, his3, trpl, ura3, can1*), and JL1-3 (genot pe like W301-1B, *aac1:LEU2 aac2:HIS3, aac3:URA*; gift from T. Drgon, NIH, Bethesda, Mar land, USA) (61), with NFV, which was followed b treatment with a Vpr-derived peptide (Genemed S nthesis Inc.) as described (62) or H_2O_2 (1 hour, 28 C). This was followed b plating on standard YPD agarose medium (200 easts/plate) and quantification of the percentage of surviving clones after 48 hours of culture at 28 C.

Liposome technology

PTPC (1 mg/ml) was separated from rat brains and ANT (0.1 mg/ml) from rat heart mitochondria as previousl described (44, 63). Immediatel after purification, pure proteins were reconstituted into proteoliposomes (phosphatid lcholine/cholesterol [5:1; wt/wt] for PTPC and phosphatid lcholine/cardiolipin [45:1; wt/wt] for ANT) (64). After e tensive dial sis to eliminate the surfactants, proteoliposomes were loaded with 4-meth llumbellifer l-phosphate (4-MUP) in 10 mM KCl, 10 mM HEPES, 125 mM saccharose (pH 7.4), b sonication (25%, 22 seconds on ice) using a Misoni 550 sonicator (Misoni Inc.), washed on Sephade PD-10 columns (Amersham Biosciences) and dispensed in 96-well microtiter plates (64). We incubated 25 μl of proteoliposomes with the indicated agents (30 minutes for NFV and 60 minutes for ATR and $Vpr_{52\ 96}$ at RT). E ternal 4-MUP was then converted to 4-meth lumbelliferone (4-MU) b the addition of alkaline phosphatase in the presence of $MgCl_2$ for 15 minutes at 37 C. The release of 4-MU was measured b spectrofluorometr (e citation 360 nm, emission 450 nm). The ma imum 4-MUP release was determined b adding 5% Triton X-100 to proteoliposomes. The percentage of 4-MUP release induced b treatment of liposomes b ATR was determined as [(ATR treated liposome fluorescence untreated liposome fluorescence)/(TX-100 treated liposome fluorescence untreated liposomes fluorescence)] × 100. The ma imal fluorescence induced b 800 μM ATR was then identified as 100% 4-MUP release, and the fluorescence induced b the treatment of liposomes b another product or another dose was calculated as a percentage of ATR-induced 4-MUP release.

Activated Bax immunofluorescence

Jurkat T cells were treated overnight with NFV or vehicle control before being induced to undergo apoptosis with 0.3 μg/ml of CH-11. Teflon-

coated 10-well immunofluorescence slides (Fischer Scientific International) were pretreated with pol -L-l sine (Pol sciences Inc.) for 1 hour at RT, washed with water, and allowed to air dr . Fift microliters of a 0.5×10^6 cell suspension was aliquoted to each well and allowed to adhere for 1 hour at 37 C. Following 1 wash with PBS, cells were fi ed with 2% paraformaldeh de and washed again with PBS. Cells were then treated with 1:250 of mouse anti-Ba (clone 6A7; BD Biosciences Pharmingen) or mouse isot pe in antibod (Santa Cru Biotechnolog Inc.) in PBS with 1 mg/ml BSA and 100 μg/ml digitonin for 1 hour at RT, followed b 2 washes with PBS. Cells were then incubated for an additional hour at RT in 1:500 of goat anti-mouse Ale a Fluor 633 (Invitrogen Corp.) and 1 mg/ml Hoechst 33342 (Invitrogen Corp.) in PBS with 1 mg/ml BSA and 100 μg/ml digitonin. Cells then underwent a final wash, were coverslipped, and imaged with laser scanning confocal microscop (LSM510; Zeiss) at an absorption/emission wavelength of 632/647 nm and 340/450 nm for Ale a Fluor 633 and Hoechst 33342, respectivel .

Computer modeling

Docking of NFV to ANT was carried out with the program QXP (65), using the FULLDOCK+ algorithm implemented in the 2003 version of the program. The recentl published cr stal structure of ANT (66) was used as the target structure. During docking, both NFV and the protein side chains were treated as totall fle ible, and the backbone atoms of the protein were allowed to move under constraints.

Statistics

Data were anal ed using the Student's *t* test for normall distributed data, ANOVA for binar variables, and the post hoc Tuke test for assessing multiple treatment groups.

Acknowledgments

A.D. Badle is supported b grants from the NIH (R01 AI62261-01-1 and R01 AI40384) and the Burroughs Wellcome Award for Translational Research (ID#1005160). S.A.L. Bennett is supported b grants from Al heimer Societ of Canada, the Canadian Institutes of Health Research (CIHR), and the Al heimer Societ of Saskatchewan. S.A.L. Bennett is a CIHR New Investi-